

UC Irvine

UC Irvine Previously Published Works

Title

Vertical profile and origin of wintertime tropospheric ozone over China during the PEACE-a period

Permalink

<https://escholarship.org/uc/item/0vb8v8bm>

Journal

Journal of Geophysical Research D: Atmospheres, 109(23)

ISSN

0148-0227

Authors

Chan, CY
Zheng, XD
Chan, LY
[et al.](#)

Publication Date

2004-12-16

DOI

10.1029/2004JD004581

Copyright Information

This work is made available under the terms of a Creative Commons Attribution License, available at <https://creativecommons.org/licenses/by/4.0/>

Peer reviewed

Vertical profile and origin of wintertime tropospheric ozone over China during the PEACE-A period

C. Y. Chan,¹ X. D. Zheng,² L. Y. Chan,¹ H. Cui,¹ E. W. L. Ginn,³ Y. K. Leung,³ H. M. Lam,¹ Y. G. Zheng,⁴ Y. Qin,⁴ C. S. Zhao,⁴ T. Wang,¹ D. R. Blake,⁵ and Y. S. Li¹

Received 29 January 2004; revised 25 June 2004; accepted 21 July 2004; published 7 October 2004.

[1] During the Pacific Exploration of Asian Continental Emission (PEACE) phase A mission in January 2002, we launched ozonesondes in subtropical southeast China at Hong Kong (114.17°E, 22.31°N), middle latitude northeast China at Beijing (116.47°E, 39.81°N), and northwest China at Xining (101.45°E, 36.43°N) in order to study long-range ozone (O₃) transport from Eurasia, tropospheric O₃ sources in China, and O₃ outflow to the Pacific. Tropospheric O₃ showed a complex vertical distribution with average tropospheric O₃ columns of 39 ± 4, 23 ± 3, and 30 ± 6 DU in Hong Kong, Beijing, and Xining, respectively, which accounted for 17 ± 2%, 7 ± 1%, and 10 ± 1% of the total O₃ column. The lower tropospheric and boundary layer (BL) O₃ over Xining and especially Beijing exhibited low values, suggesting negligible O₃ formation in middle latitudes of China during the winter season. The results also revealed frequent propagation of enhanced O₃ layers from the lower stratosphere to the upper troposphere over Xining and especially Beijing, suggesting that stratospheric O₃ is an important source of O₃ in the upper troposphere of northern China. This “natural” O₃ is transported downwind by the prevailing westerly wind and acts as a source of O₃ to the east Asian coast and northwestern Pacific. We observed elevated O₃, with a maximum mixing ratio up to 111 ppbv, at 1.5 km in the upper BL over Hong Kong. The elevated O₃ was resulted from transport of pollutants from northwest-central or southwest China and regional O₃ formation and accumulation in south China including the Pearl River Delta and Hong Kong. We also observed enhanced O₃ (>95 ppbv) in the middle and upper troposphere over Hong Kong in air masses transported along the subtropical jet from tropical and subtropical East Africa, south Asia, and Southeast Asia. The O₃ enhancements were most likely due to intrusion of stratospheric O₃ into the troposphere in the Indo-Burmese region of tropical Southeast Asia, where substantial downward motion had been

observed. **INDEX TERMS:** 0322 Atmospheric Composition and Structure: Constituent sources and sinks; 0345 Atmospheric Composition and Structure: Pollution—urban and regional (0305); 0365 Atmospheric Composition and Structure: Troposphere—composition and chemistry; 0368 Atmospheric Composition and Structure: Troposphere—constituent transport and chemistry; 0399 Atmospheric Composition and Structure: General or miscellaneous; **KEYWORDS:** tropospheric ozone, China, ozone transport

Citation: Chan, C. Y., et al. (2004), Vertical profile and origin of wintertime tropospheric ozone over China during the PEACE-A period, *J. Geophys. Res.*, 109, D23S06, doi:10.1029/2004JD004581.

1. Introduction

[2] Increasing pollutant emissions from Asia are impacting the atmospheric environment of the Asian Pacific Rim. Some recent studies show that the impact of Asian pollution

can alter the Earth's climate on a regional scale [e.g., Chan *et al.*, 2001; Menon *et al.*, 2002; United Nations Environment Programme and Centre for Clouds, Chemistry and Climate, 2002]. The PEACE mission focused on understanding chemical processes and transport of continental outflow from Asia over the western Pacific [Parrish *et al.*, 2004]. These goals cannot be achieved without knowledge of pollutant inflow from the upwind Eurasian region, and pollutant emissions and distributions within inland China. During the PEACE phase A period, in which G-2 aircraft flew over the east Asian coast and western Pacific, we performed simultaneous ozonesonde measurements of tropospheric O₃ profiles over two sites in mainland China and a site in Hong Kong. The goals were to explore possible O₃ transport from upwind Eurasia, identify the source of tropo-

¹Department of Civil and Structural Engineering, Hong Kong Polytechnic University, Hong Kong, China.

²Chinese Academy of Meteorological Sciences, Beijing, China.

³Hong Kong Observatory, Hong Kong, China.

⁴Department of Atmospheric Sciences, Peking University, Beijing, China.

⁵Department of Chemistry, University of California, Irvine, California, USA.

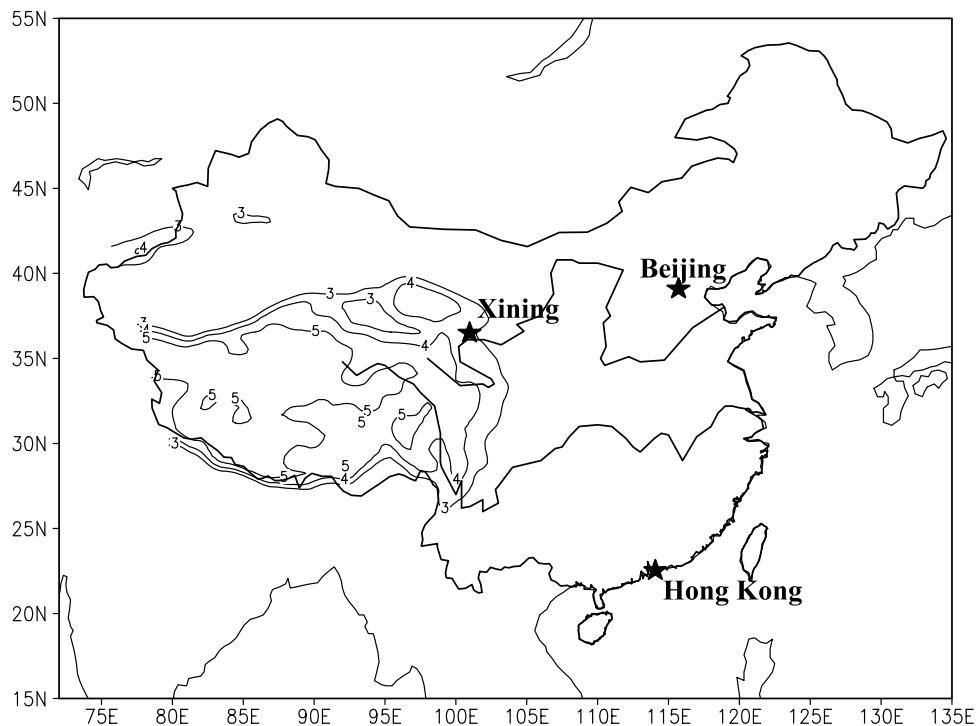


Figure 1. Map showing the ozonesonde stations in Hong Kong, Beijing, and Xining. The topography of the Tibetan plateau with altitudes higher than 3 km is shown by the contours. The unit of the contours is kilometers.

spheric O_3 over the Chinese mainland, and estimate O_3 outflow to the Pacific.

[3] The vertical distribution of O_3 in the troposphere depends on a complex interaction of O_3 exchange between the stratosphere and the troposphere, in situ photochemical O_3 formation and destruction processes, and O_3 deposition to the underlying surface. The residual tropospheric O_3 column (TOC) derived from the Total Ozone Mapping Spectrometer (TOMS) has a general minimum in the winter over the Northern Hemisphere [Fishman and Brackett, 1997]. However, satellite data over east Asia show a minimum TOC in summer [Sunwoo *et al.*, 1992]. This is somewhat different from results revealed by ozonesonde measurement in Hong Kong, which show a comparable TOC throughout summer to early winter (June–December) [Chan *et al.*, 1998; Leung *et al.*, 2004]. In Taiwan, TOC shows an obvious maximum in spring and a minimum in winter [Liu and Chang, 2001]. The TOC varies substantially in summer. However, ground-based measurements in regional background sites in east Asia, including Japan [e.g., Sunwoo *et al.*, 1994; Kajii *et al.*, 1998; Pocharnart *et al.*, 1999], mainland China [Luo *et al.*, 2000; Wang *et al.*, 2001] and Hong Kong [Lam *et al.*, 2001; C. Y. Chan *et al.*, 2002], revealed that wintertime surface O_3 in east Asia is quite high compared with that in summertime.

[4] The seasonal characteristics of tropospheric O_3 production and mixing ratios over east Asia have been investigated by a global chemical transport model [Mauzerall *et al.*, 2000]. The results suggested that maximum O_3 production in winter occurred between 20 and 30°N over east Asia. Tanimoto *et al.* [2002] reported that transport of O_3 plays a key role throughout the year in the BL over the Rishiri region of Japan. A recent modeling study suggested that the

supply and loss of BL O_3 in east Asia in winter is dominated by photochemistry [Zhang *et al.*, 2002]. Ma *et al.* [2002] reported that O_3 is produced in the winter (January) at a rate of -0.1 to 0.4 ppbv per day in the free tropospheric air and 0.0 to 1.0 ppbv per day in the mixed air over a remote inland mountain site at Waliguan Observatory, Qinghai province, China. In this paper, we present ozonesonde data observed at two stations in mainland China and a station in Hong Kong. The objectives are to investigate the characteristics of wintertime tropospheric O_3 profiles and to explore the origin of tropospheric O_3 over the Chinese mainland and western Pacific.

2. Experiment and Method

2.1. Ozonesonde Launching

[5] The three ozonesonde launching sites were located in subtropical southeast China at Hong Kong (114.17°E, 22.31°N), in midlatitude northeast China at Beijing (116.47°E, 39.81°N), and in northwest China at Xining (101.45°E, 36.43°), Qinghai Province (Figure 1). The site at Hong Kong is located in an urban area at 66 m above mean sea level (ASL). The launching site at Xining is situated in a rural area 15 km from the urban centre of Xining, at an altitude of 2296 m ASL. The site at Beijing is located in a rural area of southern Beijing, about 20 km from the perimeter of Beijing city at an altitude of 31 m ASL. The 2002 experiment was carried out from 7 to 23 January at Hong Kong, 8 to 30 January at Xining, and 10 to 23 January at Beijing. There were altogether 9, 8 and 10 ozonesondes launched in Hong Kong, Xining and Beijing, respectively. The launchings were performed from 1300 to 1400 LST (0500 to 0600 UT).

[6] Tropospheric O₃ profiles were measured by in situ electrochemical concentration cell (ECC) ozonesondes (Model 6a, Vaisala and Model 2Z, Environmental Science Corporation, EnSci) that were coupled with standard radiosondes (RS80-15GE, Vaisala) operated by a Vaisala Digi-Cora MW 15 and an EnSci portable ozonesonde receiving system. A more detailed description of the launching site at Hong Kong and Xining as well as measurement methodology and quality control procedures for each ozonesonde is given by *Chan et al.* [2003a]. The O₃ data measured by ozonesondes have precisions ranging from ±3 to 12% in the troposphere. The corresponding accuracies for individual ozonesonde soundings are ±6% near the ground, and 7 to 17% in the high troposphere, where O₃ mixing ratios are low [*Komhyr et al.*, 1995]. The integrated total column O₃ from the ozonesonde compares well with that measured by Dobson spectrophotometer with an average ratio of 1.04 ± 0.05 between the former and the latter [*Oltmans et al.*, 2001].

2.2. Backward Air Trajectory and Potential Vorticity Analysis

[7] The isentropic backward air trajectories and potential vorticity (PV) used in this study were calculated from a model developed by *Eliassen* [1987] and *Murayama et al.* [1998] using the National Centers of Environmental Prediction (NCEP) data as input. The data had a time resolution of 6 hours, horizontal resolution of 1 degree and vertical resolution of 27 layers with an interval of 50 hPa from 900 hPa to 100 hPa. In the trajectory model, an air parcel is determined to move along the transport paths of hypothetical air parcels starting at any selected isobaric surface every 6 hours. In the calculation, 1331 (11 × 11 × 11) air parcels were initially assigned to a small region with a range of ±0.5° in longitude and in latitude at a selected level over Hong Kong, Beijing and Xining. The backward air trajectories are believed to give a reasonable representation of large-scale circulation motion. They can be used to examine a potential source region of pollutants, although the exact origin of a specific air parcel cannot be determined. In the PV computation, all the meteorological elements including horizontal wind (*u*, *v*) and temperature were interpolated into standard pressure levels with a vertical resolution of about 500 m.

3. Results and Discussion

3.1. Tropospheric Ozone Column

[8] Table 1 summarizes the ozonesonde launches at the three sites during the PEACE-A period in terms of the thermal tropopause height and BL height, TOC and the contribution of TOC to total column O₃. The thermal tropopause heights and BL heights were determined from the temperature profile measured by the accompanying radiosonde, while the TOC and total column O₃ were calculated from the ozonesonde O₃ mixing ratio profile using the method described by *McPeters et al.* [1997]. The tropopause height over Hong Kong ranged from 16.0 to 18.6 km with an average and a standard deviation (same as below) of 17.5 ± 0.8 km. Compared to those over Hong Kong, the tropopause heights over Beijing and Xining were much lower ranging from 8.7 to 11.6 km ASL (10.6 ± 1.0 km) and from 7.7 to 10.1 km (8.6 ± 0.8 km), respectively. The BL height ranged from 0.6 to 2.6 km over Hong Kong, 0.4 to 2.6 km over Beijing and 0.2 to 3.4 km over

Table 1. Summary of Ozonesonde Data During the PEACE-A Period^a

	Thermal Tropopause, km									Boundary Layer Height, km						TOC, DU			Percentage of TOC to Total O ₃ Column, %								
	HK			BJ			XN			HK			BJ			XN			HK			BJ			XN		
	HK	BJ	XN	HK	BJ	XN	HK	BJ	XN	HK	BJ	XN	HK	BJ	XN	HK	BJ	XN	HK	BJ	XN	HK	BJ	XN			
7 Jan.	16.7	–	–	2.2	–	–	47	–	–	20	–	–	–	–	–	–	–	–	–	–	–	–	–	–			
8 Jan.	–	–	8.3	–	–	0.2	–	–	22	–	–	–	–	–	–	–	–	–	–	–	–	–	–	8			
9 Jan.	16.0	–	9.4	0.6	–	0.3	39	–	28	16	–	–	–	–	–	–	–	–	–	–	–	–	–	9			
10 Jan.	–	11.2	–	–	2.4	–	–	22	–	–	–	–	–	–	–	–	–	–	–	–	–	–	–	6			
11 Jan.	18.1	11.6	–	2.2	0.4	–	34	22	–	14	8	–	–	–	–	–	–	–	–	–	–	–	–	–			
13 Jan.	18.6	10.6	10.1	1.7	1.5	0.7	40	28	32	17	10	11	–	–	–	–	–	–	–	–	–	–	–	–			
15 Jan.	17.6	11.5	–	2.6	2.1	–	35	22	–	16	8	–	–	–	–	–	–	–	–	–	–	–	–	–			
17 Jan.	18.2	11.0	8.7	1.5	1.2	2.1	38	21	27	17	6	10	–	–	–	–	–	–	–	–	–	–	–	–			
19 Jan.	17.8	9.8	8.3	2.6	0.4	3.4	38	22	31	17	7	10	–	–	–	–	–	–	–	–	–	–	–	–			
21 Jan.	17.5	8.7	8.2	1.4	2.6	1.1	38	22	34	17	6	12	–	–	–	–	–	–	–	–	–	–	–	–			
23 Jan.	17.3	10.1	7.8	1.4	1.3	1.5	41	27	27	18	9	9	–	–	–	–	–	–	–	–	–	–	–	–			
25 Jan.	–	–	7.7	–	–	1.9	–	–	30	–	–	–	–	–	–	–	–	–	–	–	–	–	–	–			
28 Jan.	–	–	7.7	–	–	1.7	–	–	28	–	–	–	–	–	–	–	–	–	–	–	–	–	–	–			
30 Jan.	–	–	9.5	–	–	1.1	–	–	43	–	–	–	–	–	–	–	–	–	–	–	–	–	–	–			
Average	17.5	10.6	8.6	1.8	1.5	1.4	39	23	30	17	7	10	–	–	–	–	–	–	–	–	–	–	–	–			
SD	0.8	1.0	0.8	0.7	0.8	1.0	4	3	6	2	1	1	–	–	–	–	–	–	–	–	–	–	–	–			

^aHK, Hong Kong; BJ, Beijing; XN, Xining. SD, standard deviation. Dashes indicate no sounding.

Xining. The respective average values were 1.8 ± 0.7 km, 1.5 ± 0.8 km and 1.4 ± 1.0 km above ground surface.

[9] The TOC over Hong Kong ranged from 34 to 47 DU with an average of 39 ± 4 DU. These values accounted for 14–20% and $17 \pm 2\%$ of the total column O₃. The TOC over Xining ranged from 22 to 43 DU (an average of 30 ± 6 DU), which accounted for 8–13% ($10 \pm 1\%$) of the total O₃ column, while the TOC over Beijing (21–28 DU; average of 23 ± 6 DU) accounted for 6–10% ($7 \pm 1\%$) of the total column O₃. The TOCs measured over Hong Kong during the PEACE-A period are comparable to the climatological monthly value for January from 1994 to 2002 (42 ± 7 DU). They are also close to the values observed in January from 1994 to 1999 over Taipei (25°N, 121.3°E) [*Liu and Chang*, 2001]. The TOCs measured over Xining during PEACE-A were in the lower half of the range reported for summer months. *Zheng* [2000] reported that the TOC from the surface to 100 hPa altitude over Xining in the summer of 1996 ranged from 20 to 60 DU. The lower TOC over Beijing and Xining than over Hong Kong is due to the fact that the tropospheric columns over Beijing and Xining were shallower as they are situated at high latitudes. Xining is located on the high-altitude Tibetan Plateau at comparable latitude with Beijing. A relatively lower TOC has been observed over high-altitude regions around the world when compared with those in similar latitude regions [e.g., *Zhou et al.*, 1995; *Zou*, 1996; *Fishman and Brackett*, 1997]. However, in this study, the TOC over Xining was higher than that over Beijing as was the percentage contribution of TOC to the total column O₃. This suggests that there were other possible causes leading to the low TOC over Beijing.

3.2. Characteristics of Tropospheric Ozone Profiles and Distributions

[10] There are substantial differences in the characteristics of the vertical O₃ distribution in the troposphere among the three sites. Figure 2 shows the respective time-height cross sections of O₃ mixing ratios. Also included in this figure are

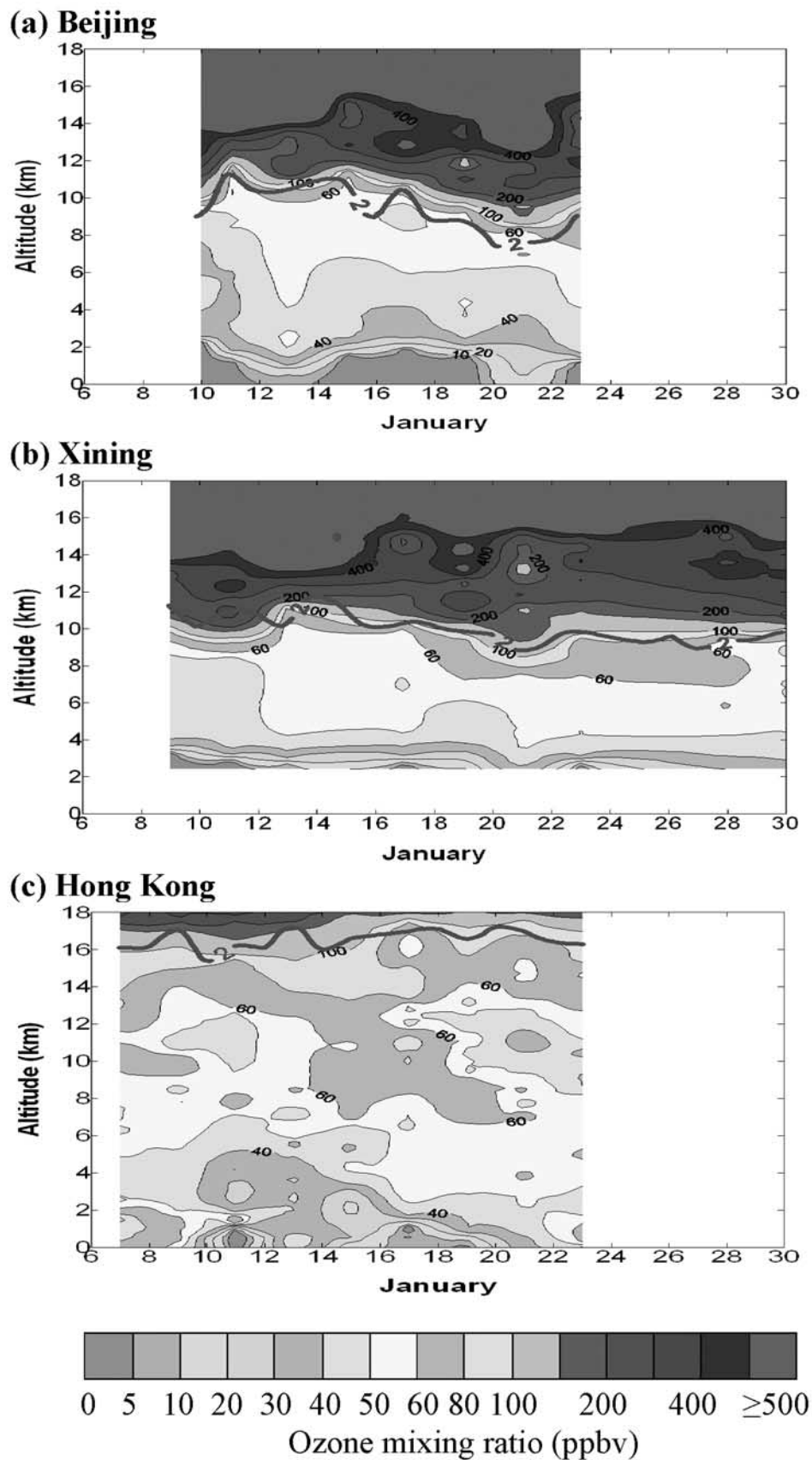


Figure 2. Time-height contour of ozone mixing ratio (ppbv) for (a) Beijing, (b) Xining, and (c) Hong Kong during the PEACE-A period. The dynamical tropopauses are identified by 2 unit lines of potential vorticity (PVU, $1 \text{ PVU} = 1 \times 10^{-6} \text{ s}^{-1} \text{ m}^2 \text{ kg}^{-1}$). See color version of this figure at back of this issue.

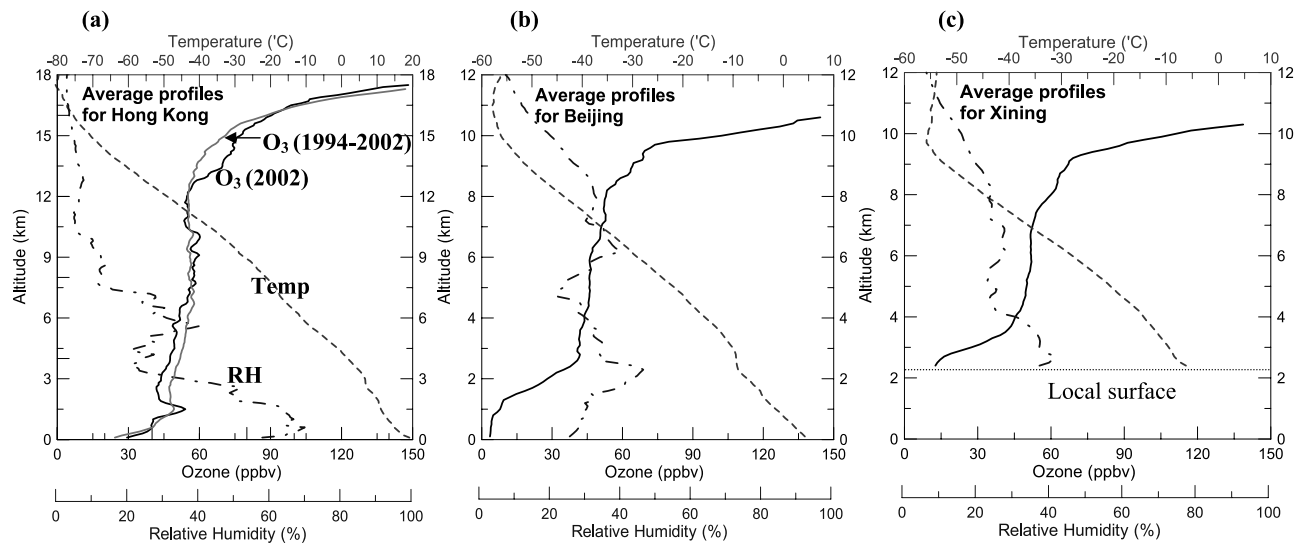


Figure 3. Average vertical profiles of ozone mixing ratios (ppbv) (solid line), relative humidity (%) (dash-dotted line), and temperature ($^{\circ}\text{C}$) (dashed line) for (a) Hong Kong, (b) Beijing, and (c) Xining during the PEACE-A period. The grey solid line in Figure 3a is the mean ozone profile for January from 1994 to 2002. The horizontal line in Figure 3c is the altitude of the local surface.

the surfaces with potential vorticity units (PVU) equal to 2, which are commonly referred to as a dynamical definition of tropopause in the middle latitudes [Holton *et al.*, 1995; Folkins and Appenzeller, 1996; Kim *et al.*, 2002]. Figure 3 shows the average profiles of O_3 mixing ratios, RH and temperature in the troposphere over Hong Kong, Beijing and Xining for the PEACE-A period. We note that the Xining altitude profiles show sea level at 0 km, whereas the local surface begins at 2.3 km. The average O_3 profiles and distributions over Beijing and Xining shared a similar pattern, with low O_3 mixing ratios of less than 45 ppbv in the BL and moderate O_3 levels in the 40–60 ppbv range in the middle troposphere. In the upper troposphere, O_3 mixing ratios showed a sharp increase up to the tropopause. The average O_3 levels over Beijing had values less than 5 ppbv below 1.0 km before picking up a sharp increase from around 10 ppbv at 1.2 km to ~ 40 ppbv at 3.0 km, from where it showed a small increase to ~ 50 ppbv at 8.0 km. Ozone profiles over Xining increased from the BL to around 9.5 km before a much sharper increase at the higher altitudes.

[11] Ozone mixing ratios over Hong Kong had a more complex profile and distribution compared to that of Beijing and Xining. A much higher O_3 mixing ratio was found in the BL. Ozone usually had a mixing ratio of less than 50 ppbv below 5 km from 7 to 16 January and below 2.5 km from 16 to 23 January (Figure 2). It had a local maximum from 7 to 11 January in the BL, with the mixing ratio reaching 100 ppbv. The average O_3 profile had a prominent local O_3 peak with a maximum mixing ratio of 55 ppbv in the midBL around 1.2 km (Figure 3). The O_3 mixing ratio increased steadily from ~ 40 ppbv at 2.0 km to around 60 ppbv at 10 km. Ozone had a mixing ratio of 50–70 ppbv between 5 and 12 km from 7 to 14 January, and 40–100 ppbv between 5 and 14 km from 14 to 23 January. It had a local peak from 13 to 21 January in the middle and upper troposphere (6.6–12 km) with maximum O_3 mixing ratios greater than 100 ppbv. It also showed a relative minimum centered at 10–13 km before a steady increase to the

tropopause. Figure 3a also shows the monthly mean O_3 profile in Hong Kong for January averaged from 1994 to 2002 for comparison. We note that the general features of the average O_3 profile at Hong Kong for PEACE-A were similar, with an exception in the BL, to those displayed by the long-term average profile. This shows that the measurements during the PEACE-A period may reflect the typical situation in January.

[12] The wintertime O_3 profiles over Beijing and Xining look quite similar to those over midlatitude coastal east Asia at Sapporo (43.1°N , 141.3°E) and Tsukuba (36.1°N , 140.1°E) in Japan, and midlatitude coastal west United States at Trinidad Head (40.8°N , 124.2°N), California, the United States. In particular, O_3 in winter (December–February) in these Japanese and U.S. stations shows quite steady mixing ratios of 40–60 ppbv in the free troposphere and sharp increases in the upper troposphere at around 9–11 km [Oltmans *et al.*, 2004], similar to those over Beijing and Xining (Figure 3). However, we noted that O_3 in the lower troposphere and BL of Beijing is considerably lower than those (25–50 ppbv) at Sapporo, Tsukuba and Trinidad Head. The O_3 profiles over Beijing and Xining are also much different from that in tropical Asia at the Malaysia Peninsula, where wintertime O_3 shows substantial variations throughout the troposphere [Yonemura *et al.*, 2002].

3.2.1. Origin and Source of Ozone in the Boundary Layer

[13] As discussed above, O_3 in the BL over Beijing and Xining showed very low mixing ratios for most of January 2002 (Figure 3). In particular over Beijing, O_3 mixing ratios dropped to very low values in most profiles (not shown). This is reasonable as winter, especially in high latitudes, is not a season with favorable meteorological conditions for photochemical O_3 production. During PEACE-A, the weather in northern China was usually cloudy, with limited sunshine and quite cold. The average temperature during the launching period (1300–1400 LST), which can be considered close to the average daily maximum temperature as

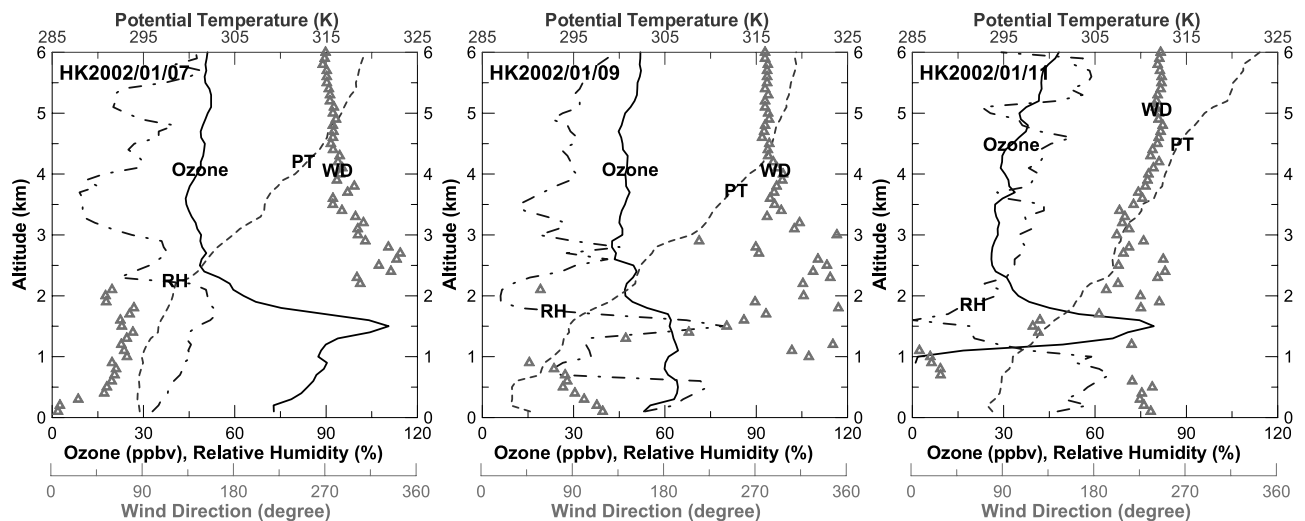


Figure 4. Vertical profiles of ozone mixing ratios (ppbv) (solid line), relative humidity (%) (dash-dotted line), potential temperature (K) (dashed line), and wind direction (degrees) (triangles) over Hong Kong on 7, 9, and 11 January 2002.

revealed by radiosonde temperature profiles was below 5°C over Beijing and -5°C over Xining (Figure 3). Again, we note that the altitude of the Xining site is 2.3 km above sea level, and that 0 km represents sea level in Figure 3. At such low solar radiation and temperatures, photochemical production of O_3 was limited. Thus it is more likely higher O_3 in Hong Kong than in Beijing/Xining is driven by more availability of solar radiation owing to the low latitude of Hong Kong. The higher O_3 in Hong Kong than that in Xining is also likely due to higher latitudinal O_3 production tendency as a result of higher available solar radiation. This is consistent with the model results reported by *Mauzerall et al.* [2000] that net O_3 production tendency is positive in low latitude in Asia while negative in higher-latitude zones.

[14] However, the nearly zero O_3 levels in the BL especially over Beijing suggest that there were additional causes of O_3 depletion. This low regional O_3 is most probably due to chemical titration of O_3 by freshly emitted nitrogen oxide (NO) from vehicular exhaust and, to a lesser extent, dry deposition of O_3 to the underlying surface. There are over 2 million vehicles in Beijing city [*Zhao and Gallagher, 2003*]. The large amount of NO emitted from these vehicles is believed to be the major cause of the low O_3 observed in Beijing. *Zheng et al.* [2002] reported that surface NO concentrations at an urban site in Beijing usually reached over 100 ppb in the daytime and can reach over 700 ppb. The number of vehicles in Xining (less than 0.1 million) and Hong Kong (around 0.5 million) [*L. Y. Chan et al., 2002*] are

much lower, and thus the titration of O_3 at these two sites was less noticeable. Hence the O_3 mixing ratios were higher in the BL over Xining and Hong Kong. Such chemical titration of O_3 by NO has also been observed by ozonesonde and ground-based measurements in many cities including Hong Kong and Calgary, Canada, for examples [*Angle and Sandhu, 1988; Chan et al., 1998; Yeung et al., 1996*].

[15] We observed enhanced O_3 layers in the BL in early January over Hong Kong (Figures 2 and 3). For example, Figure 4 shows the vertical profiles of O_3 mixing ratio, RH, potential temperature (PT) and wind direction below 6 km for 7, 9, and 11 January 2002 over Hong Kong. The O_3 mixing ratio was greater than 70 ppbv close to the surface on 7 January. It increased sharply to reach a local peak of 90 ppbv at 0.9 km before climbing to a maximum of 111 ppbv at 1.5 km. The O_3 enhancement was much less noticeable by 9 January, with O_3 mixing ratios of 45–62 ppbv below 2.0 km. On 11 January, O_3 mixing ratios reached a peak of 80 ppbv at 1.7 km. Similarly to 7 January, the O_3 mixing ratio began to drop until above a temperature inversion located at around 2.0 km, which defined the top of the BL. The elevated O_3 was usually accompanied by moderate to high RH. There were noticeable temperature inversions at 0.6–0.7 km, especially on 9 and 11 January (Figure 4), and there were obvious decreases in RH and changes in temperature in the elevated O_3 layer, especially on 11 January. Notably, there was a change in wind direction from the east to northeast on 7 and 9 January to the north to northwest on 11 January in the

Table 2. Selected Meteorological Observations for Hong Kong, January 2002

Date	Air Temperature, $^{\circ}\text{C}$			Total Bright Sunshine, hours	Daily Global Solar Radiation, MJ/m^2	Mean Dew Point $^{\circ}\text{C}$	Mean Amount of Cloud, %	Prevailing Wind	
	Maximum	Mean	Minimum					Wind Direction, deg	Mean Wind Speed, km/h
7 Jan.	22.2	19.2	16.5	8.3	11.49	13.2	6	060	4.9
9 Jan.	17.8	17.0	15.7	9.0	14.33	12.5	32	060	30.3
11 Jan.	22.0	19.2	16.9	8.4	12.42	15.8	18	230	5.1
Monthly	19.3	17.3	15.5	161.9	10.11	12.7	55	020	20.0
Mean/Total									
Normal	18.6	15.8	13.6	152.4	11.63	10.2	58	070	24.0

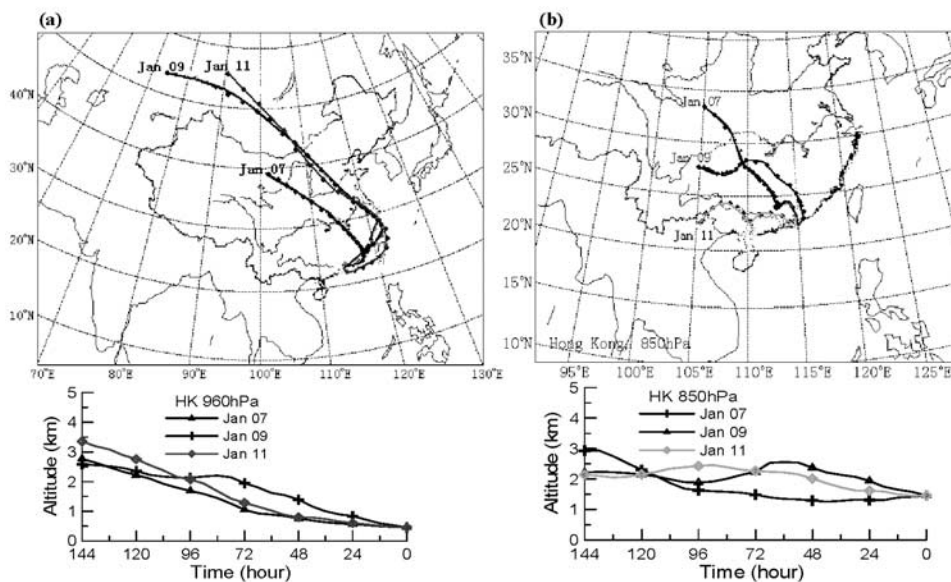


Figure 5. Five-day backward air trajectories reaching Hong Kong at (a) 960 hPa (~0.5 km) and (b) 850 hPa (~1.5 km) on 7, 9, and 11 January 2002. See color version of this figure at back of this issue.

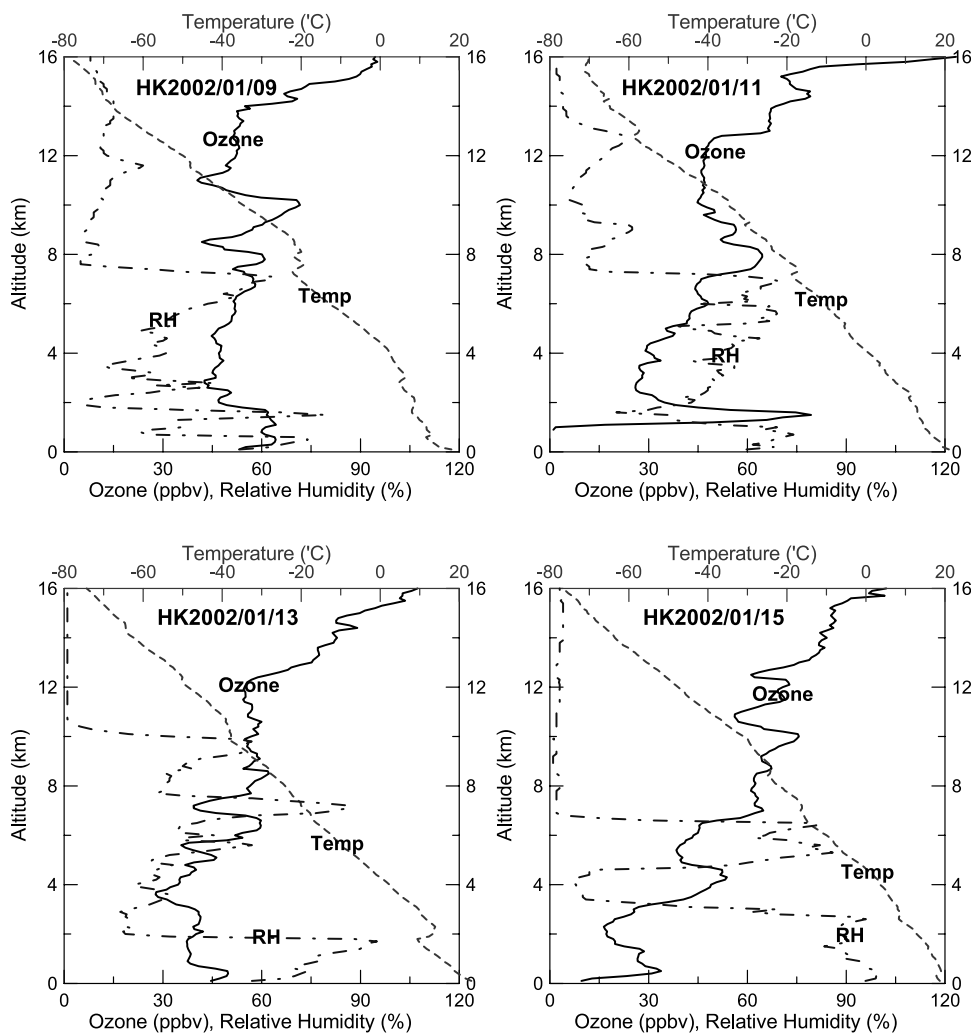


Figure 6. Vertical profiles of ozone mixing ratios (ppbv) (solid line), relative humidity (%) (dash-dotted line), and temperature (°C) (dashed line) over Hong Kong from 9 to 23 January 2002.

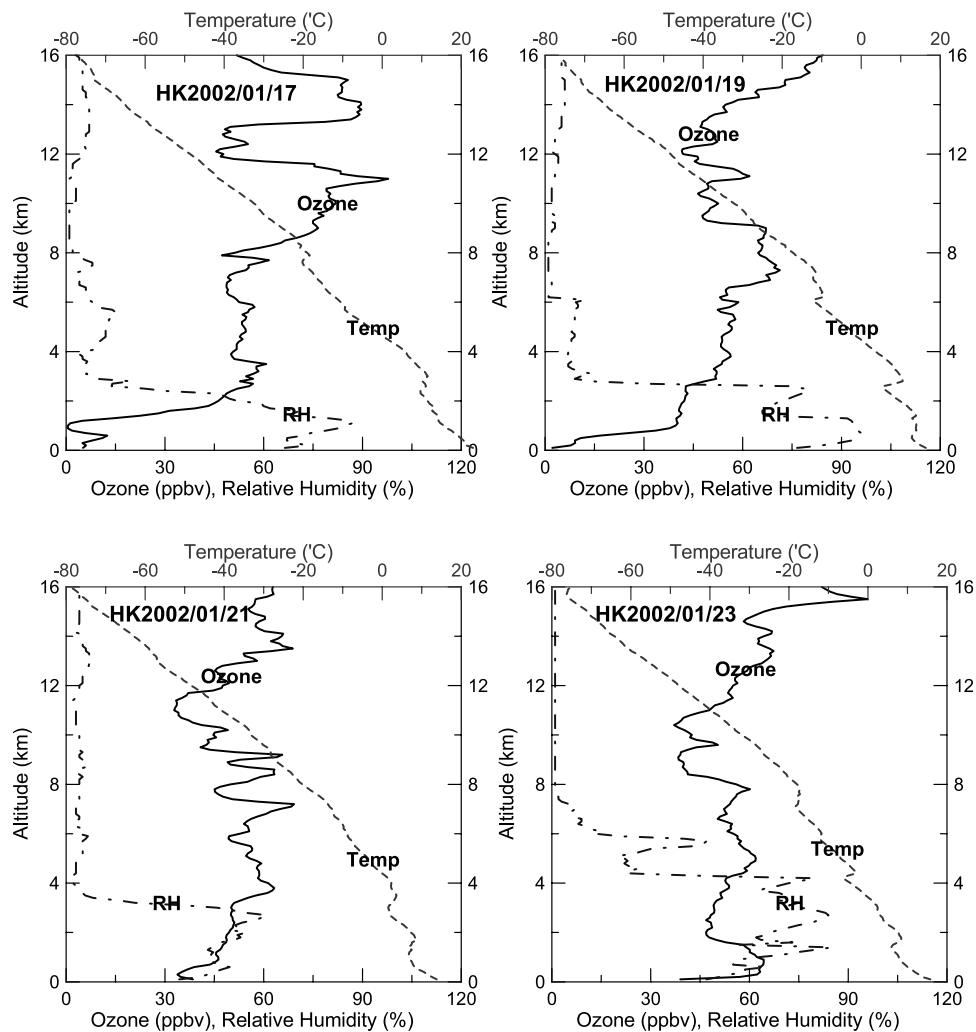


Figure 6. (continued)

BL (see also Table 2). The wind in the BL also distinguished itself from the prevailing westerly wind in the free troposphere by a sharp change in wind direction. Wang *et al.* [2003] reported measurements of O_3 , NO_y , CO and SO_2 obtained during October 2001 to January 2002 from a rural site in western Hong Kong. The mixing ratio of O_3 close to the ground surface was only about 40 ppbv on 7 January (compared to over 70 ppbv at 1.7 km in our measurement site in urban Hong Kong on 7 January; Figure 4, left panel).

[16] The enhanced O_3 measured by ozonesondes in this study was situated at a lower altitude when compared with that typically found in springtime over the lower troposphere at 2.5–6 km over Hong Kong [Chan *et al.*, 2000, 2003b]. The east Asian region in this period was under the influence of a weak to moderate high-pressure system that moved in a southeasterly direction from northwestern Asia on 7 January to over the central-eastern China coast on 9 and 11 January. The system resulted in a continental airflow from the high latitudes of northwestern China to southeastern China, with accompanying sunny and dry weather in the region (Table 2). There was also a stagnant atmosphere with a daily mean wind speed around 5 km/h (1.4 m/s) in Hong Kong on 7 and 11 January (Table 2). Figure 5 shows the backward air trajectories of the air masses reaching Hong

Kong at 850 and 960 hPa altitudes on 7, 9, and 11 January. The trajectories at 960 hPa (~ 0.5 km) (Figure 5a) originated from high latitudes of northwestern China. They traveled in a southeastern direction before turning into a northeastern direction over the central eastern or southeastern China coast 1–3 days before reaching Hong Kong.

[17] C. Y. Chan *et al.* [2002] reported that air masses associated with these types of trajectories had surface O_3 concentrations of 40–50 ppb, comparable to those measured by the ozonesondes in this study. The O_3 -rich air masses at 850 hPa (~ 1.5 km) on 7 and 9 January also originated from northwestern China. They however traveled more directly in a southeastern direction across central and south China before reaching Hong Kong (Figure 5b). On 11 January, the air mass had originated from southwest China and had traveled over the Guangxi Province prior to passing over the industrialized Pearl River Delta (PRD) of the Guangdong Province the day before reaching Hong Kong. The transport of O_3 from the heavily polluted PRD has been identified as an important cause of surface O_3 episodes in Hong Kong [Chan and Chan, 2000; Wang *et al.*, 2003]. The surface wind records showed that there was a change of wind (from the west) on 11 January (Table 2). Judging from the regional meteorological conditions, we

believe that the elevated O_3 levels were the result of transport of pollutants from northwest-central or southwest China and regional photochemical O_3 formation in south China. However, low-latitude regions are very active in convective upward transport in general and thus we cannot exclude the contribution of O_3 of Hong Kong local origin to the enhanced O_3 on 7 and 11 January.

3.2.2. Origin and Source of Ozone in the Middle and Upper Troposphere

[18] We noted that there were substantial changes in O_3 mixing ratios in the middle and upper troposphere over Hong Kong, with a local minimum at the beginning and the end of the experiment period, and a local maximum centered on 17 January. Figures 6a–6b shows the vertical profiles of O_3 mixing ratios, RH and temperature over Hong Kong from 11 to 23 January. The O_3 mixing ratio started to increase on 13 January and reached its maximum on 17 January with an enhanced layer at 8–12 km. A maximum O_3 mixing ratio of 98 ppbv was found at 11 km on 17 January. The O_3 mixing ratio in the layer noticeably decreased by 19 January and the O_3 mixing ratio reached a minimum toward the end of the period. The O_3 in the enhanced layer was isolated from the O_3 above it by an O_3 decrease between 12 and 13 km. The enhanced O_3 was accompanied by very low specific humidity (<0.1 g/kg) and PV (0.4 PVU) (not shown). Whereas the low specific humidity suggests that the O_3 -rich air masses might have originated from the stratosphere, the accompanying low PV tends to suggest that intrusion of O_3 from the stratosphere over Hong Kong was not the source of O_3 in the enhanced layer.

[19] The O_3 -enhanced air masses were accompanied by a westerly wind (not shown). Backward air trajectories suggest that the O_3 -rich air masses had originated over eastern Africa and the southern Arabian Peninsula, then traveled over the Arabian Sea in their early journey before passing over central India. The air masses then traveled over the Bay of Bengal and the northern Indochina Peninsula before reaching south China and Hong Kong (Figure 7). The air masses, especially at 375 hPa and 1–2 days before reaching Hong Kong, had undergone noticeable downward motion. Enhanced CO mixing ratios were observed over eastern Africa, the southern Arabian Peninsula, the Indian Peninsula and the SE Asian subcontinent, especially at 850 and 700 hPa altitudes by the Measurements of Pollution in the Troposphere (MOPITT) instrument on board of a satellite (www.eos.ucar.edu/mopitt) and to a much lesser extent at 500 hPa. An analysis of outgoing longwave radiation (OLR) (www.cdc.noaa.gov/cdc/data.interp_OLR.html) suggests that there was enhanced OLR and thus suppressed convective activity in these regions. These conditions were unfavorable for transport of pollutants vertically to higher altitudes where they could be transported horizontally to south China and Hong Kong by westerly winds. We thus believe that the O_3 enhancements were not the result of transport of photochemical O_3 produced from emission sources that caused the elevated CO in the SE Asian and Indian regions.

[20] Figure 8 shows the distributions of PV, wind vectors and pressure vertical velocity over Asia on 15 January 2002. Noticeably, there was a sharp PV gradient along the subtropical jet stream around 20° – 30° N latitude, which is the location where active stratospheric-tropospheric exchange of O_3 occurs [Shapiro *et al.*, 1982; Uccellini *et*

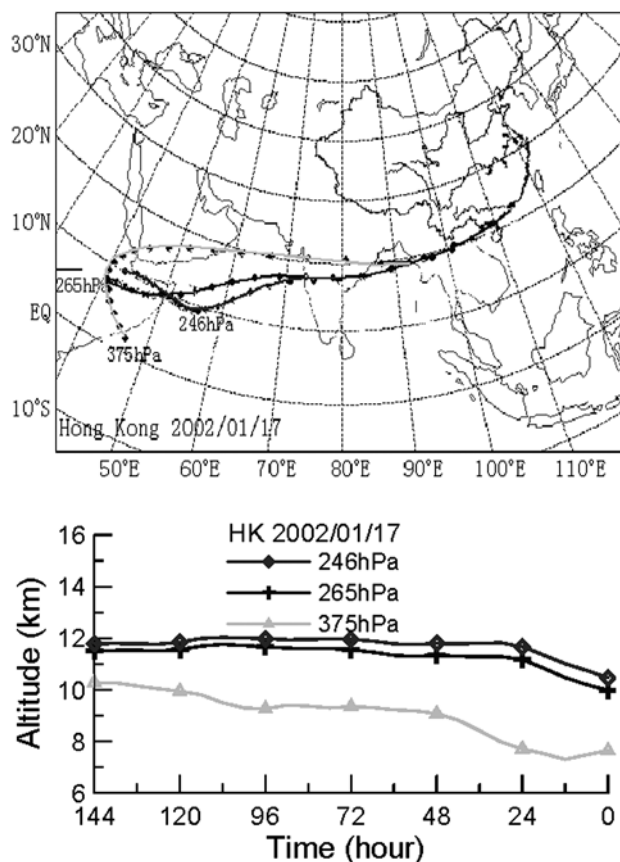


Figure 7. Five-day backward air trajectories reaching Hong Kong at 375, 265, and 246 hPa on 17 January 2002. See color version of this figure at back of this issue.

al., 1985]. Chan *et al.* [2003a] showed that the active stratospheric-tropospheric exchange of O_3 associated with tropopause folding at the subtropical jet stream is the cause of tropospheric O_3 enhancements over middle latitudes of central-eastern China. There was also substantial subsidence over the Indo-Burmese region of SE Asia where O_3 -rich air masses had passed over. These suggest that the enhanced O_3 observed over the middle and upper troposphere of Hong Kong between 13 and 21 January was due to intrusion of stratospheric O_3 in the high altitudes of Indo-Burmese region of SE Asia.

[21] We also observed relatively low O_3 over Hong Kong in the middle and upper troposphere at around 8–13 km from 9 to 12 January and from 17 to 23 January (Figure 2). The lowest O_3 mixing ratio reached 40–50 ppbv and 30–40 ppbv, respectively. The vertical profiles (Figures 6a–6b) showed that the depleted O_3 layer was located between 10.5 and 14 km on 9 January and 10 and 13 km on 11 January. Within these layers, the O_3 mixing ratio usually showed relatively lower values than at intermediate altitudes. The depleted layers, especially on 23 January, were lower than 10 km in altitude with a local O_3 minimum located between 8.3 and 10.6 km. Chan *et al.* [1998] and Newell *et al.* [1997] associated these low- O_3 events with the transport of O_3 -depleted air from the tropical SE Asian region following the east Asia local Hadley circulation. The backward air trajectories (Figure 9) suggest that the O_3 -depleted air

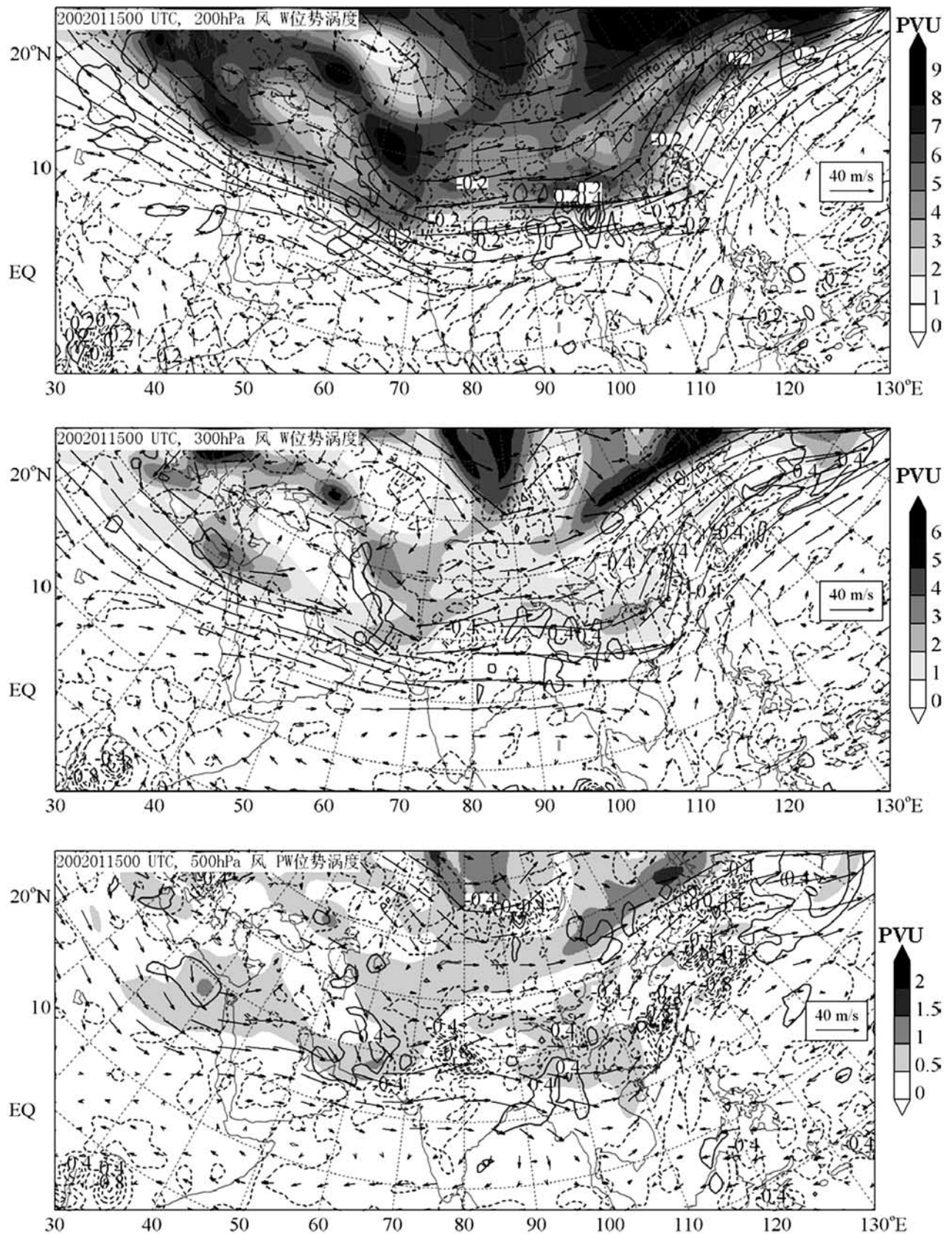


Figure 8. Distribution of potential vorticity (PVU) (shaded), pressure vertical velocity (Pa/s) (solid lines for positive, downward motion and dashed lines for negative, upward motion), and wind vector (m/s) (arrows) over Asia at 200, 300, and 500 hPa on 15 January 2002. See color version of this figure at back of this issue.

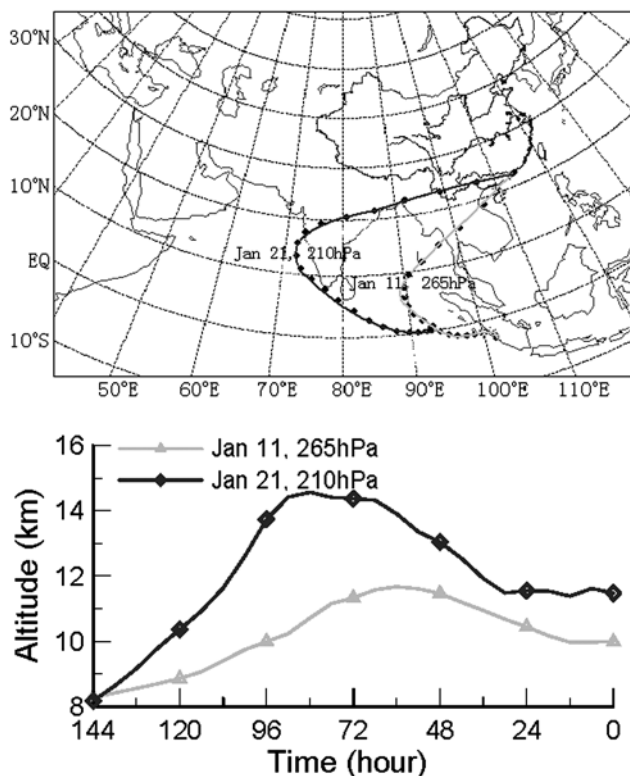


Figure 9. Five-day backward air trajectories reaching Hong Kong at 265 hPa on 11 January 2002 and at 210 hPa on 21 January 2002. See color version of this figure at back of this issue.

masses originated from the tropical Indonesian region. They flowed over south Asia or SE Asia before reaching south China and Hong Kong. We note that there was substantial upward movement of air masses to the upper troposphere, especially on 21 January over the equatorial Pacific, before noticeable sinking movements over the Indian Peninsula and SE Asian subcontinent 2–3 days before reaching Hong Kong. The backward air trajectories suggest that the low O_3 was due to the long-range transport of maritime air from the tropical SE Asian region.

[22] Figure 2 shows that O_3 in the upper troposphere above Beijing and Xining during the PEACE-A period followed the propagation of surfaces with $PVU = 2$ from higher altitudes at the beginning of the period to lower altitudes at the end of the period. Noticeably, there were sharp O_3 gradients from the upper troposphere toward the tropopause over Beijing. An examination of the O_3 mixing ratios, PT and PV profiles in the upper troposphere revealed that there were simultaneous increases in O_3 mixing ratio, PT and PV just below the tropopause. Figure 10 shows selected profiles of O_3 mixing ratios, specific humidity, PT and PV over Xining and Beijing. We note that there was always a sharp increase in O_3 mixing ratios, PT and PV as well as a decrease in specific humidity from around 8 km to the altitudes at which the $PVU = 2$, the dynamical tropopause. The O_3 , PT and PV enhancements over Beijing were more noticeable than those over Xining.

[23] Also, there were frequent advections of layers of high O_3 mixing ratios from the lower stratosphere to the

troposphere over Beijing and Xining, such as the ones displayed in Figure 10. Such advections of O_3 laminae have been associated with the stratospheric-tropospheric exchange of O_3 through tropopause folding over Japan [Austin and Midgley, 1994], Korea [Kim et al., 2002] and central-eastern China [Chan et al., 2003a] in the spring. Zheng et al. [2001] also reported an intrusion of stratospheric O_3 through tropopause folding with a similar advection of O_3 layers over Beijing in the summer of 1999. The simultaneous O_3 , PT and PV increases and the advection of O_3 layers suggest that stratospheric O_3 was an important source of O_3 in the upper troposphere over Beijing and Xining during the PEACE-A period. Previous studies have also suggested that diffusion processes associated with jet streams following tropopause folding also lead to transport of stratospheric O_3 to the troposphere [Austin and Midgley, 1994; Tsutsumi and Makino, 1995]. Figure 11 shows the pressure vertical velocity for east Asia at 300 and 500 hPa averaged over the PEACE-A period. This figure together with case-by-case analysis suggested that there was persistent subsidence and high PV over north China, especially its northeastern part including the Beijing and Xining regions, which were located poleward of the jet entrance region. Such subsidence and high PV may imply there were frequent occurrences of tropopause folding or intrusion events and hence the vertical transport of stratospheric O_3 to lower altitudes of the troposphere. Superimposed on the pressure vertical velocity in Figure 11 are wind vectors. Judging from the wind fields, the stratospheric O_3 transported into the troposphere was further transported to the downwind regions of the east Asian coast and northwestern Pacific. This “natural” O_3 is thus an important source of O_3 in these downwind regions.

4. Conclusions

[24] Our measurements during the PEACE-A period reveal complex O_3 distributions in the troposphere over subtropical and midlatitude China, although the measurements covered only a short period of time. Ozone levels in the lower troposphere and BL over Xining and especially Beijing had low values, suggesting that there is negligible O_3 formation at midlatitudes of China during the winter. The overall low TOC over Beijing is caused by additional loss of O_3 in the BL and lower troposphere, which is probably related to the chemical titration of O_3 by freshly emitted NO from the large number of vehicles. Such hypothesis however has to be further tested with measurement data or chemical modeling. We observed elevated O_3 layers in the upper BL over Hong Kong, due to transport of pollutants from northeast-central or southwest and regional O_3 formation and accumulation in south China including the PRD and Hong Kong. The results also revealed frequent propagation of enhanced O_3 layers from the lower stratosphere to the upper troposphere over Xining and especially Beijing. This stratospheric O_3 is an important source of O_3 in the upper troposphere of northern China as well as the east Asian coast and northwestern Pacific. We also observed O_3 enhancements in the middle and upper troposphere over Hong Kong in air masses transported along the subtropical jet stream from tropical and subtropical East Africa, south Asia, SE Asia and south China. Our analysis suggested that

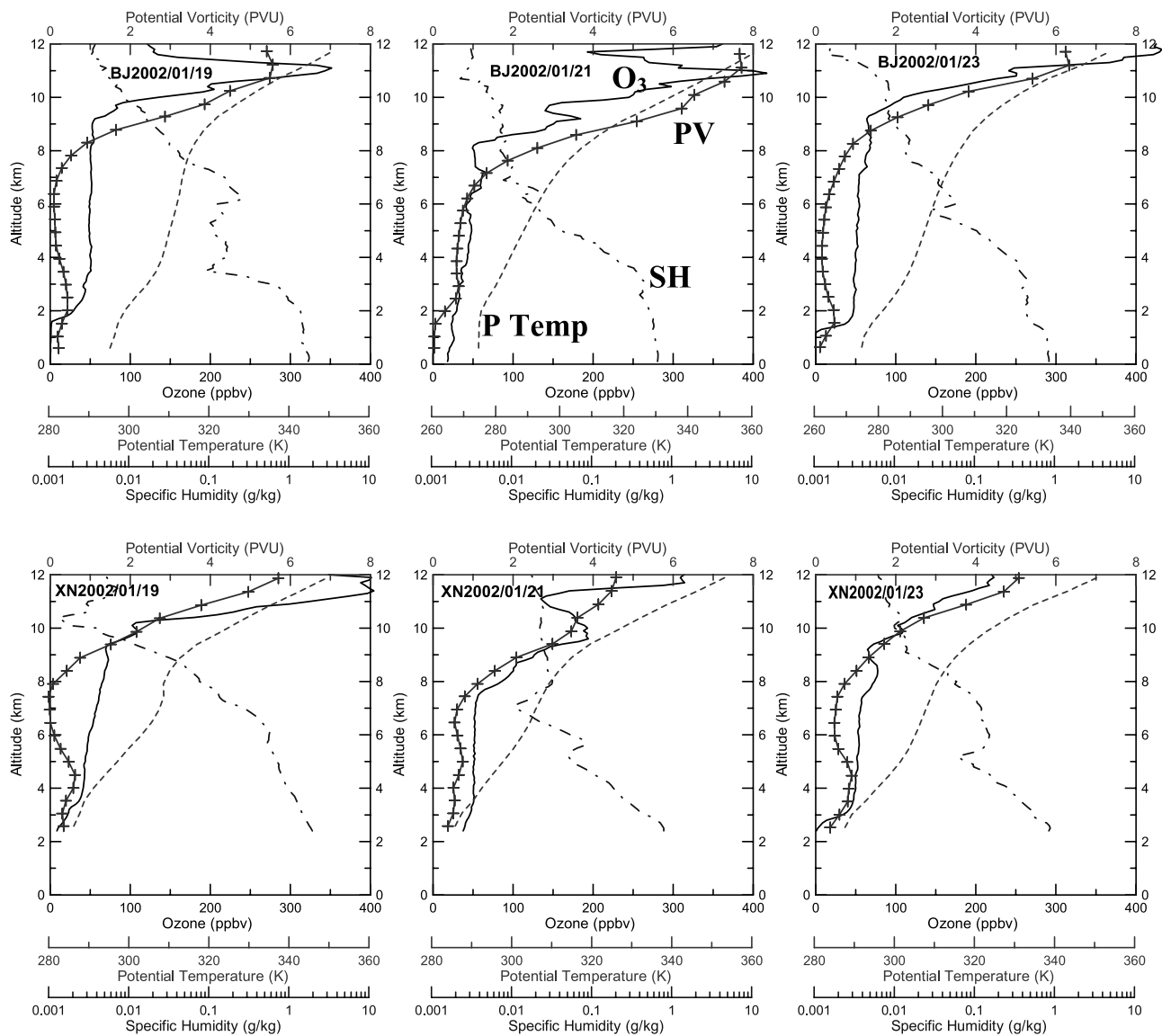


Figure 10. Vertical profiles of ozone mixing ratios (ppbv) (solid line), specific humidity (g/kg) (dash-dotted line), potential temperature (K) (dashed line), and potential vorticity (PVU) (line with crosses) over Beijing and Xining on 19–23 January 2002.

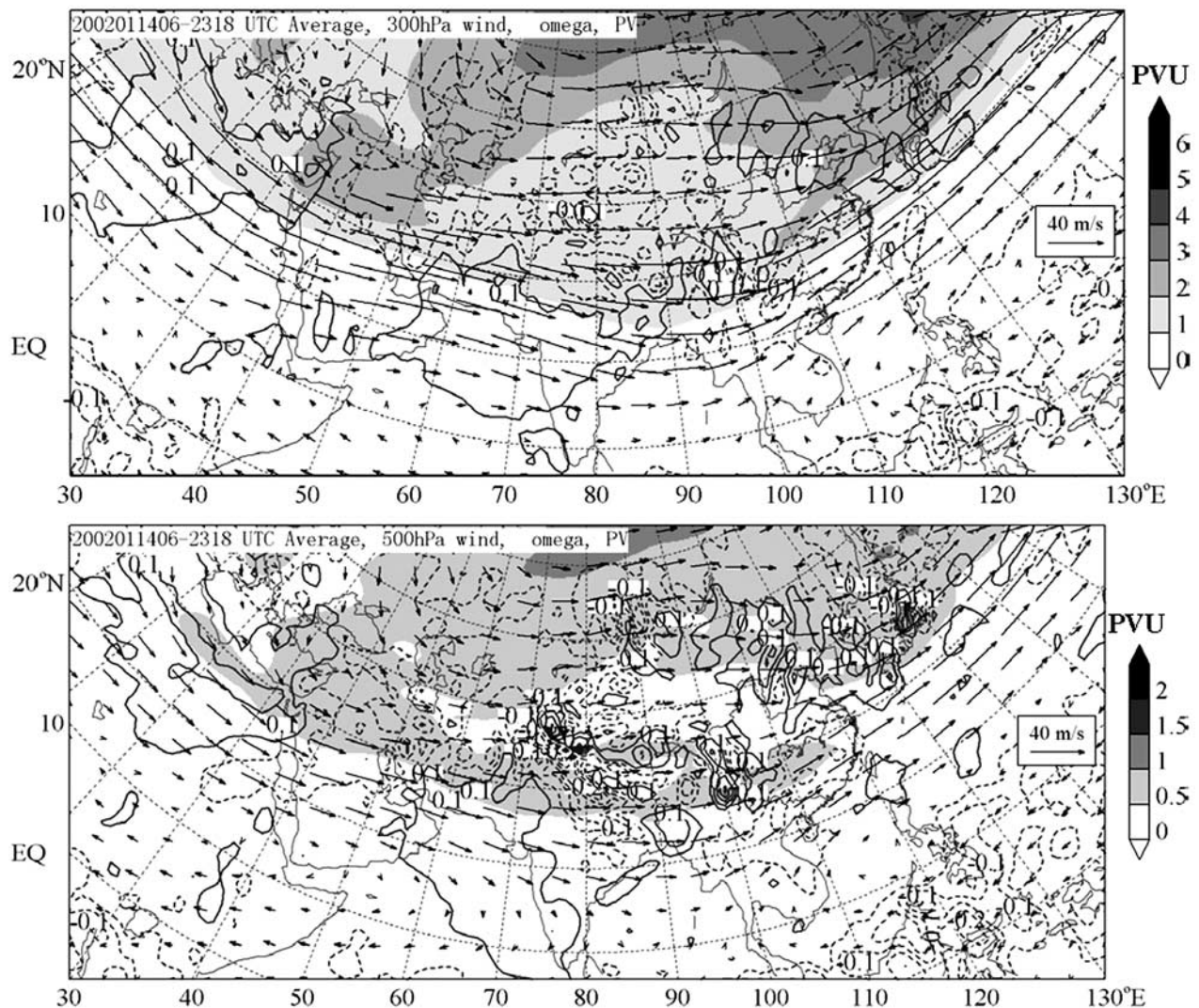


Figure 11. Mean potential vorticity (PVU) (shaded), pressure vertical velocity (Pa/s) (solid lines for positive, downward motion and dashed lines for negative, upward motion), and wind vector (m/s) (arrows) over Asia at 500 and 300 hPa averaged over the period from 6 to 23 January 2002. See color version of this figure at back of this issue.

these enhancements were due to intrusion of stratospheric O_3 from the Indo-Burmese region of SE Asia, where subsiding downward motion was observed. This study showed that stratospheric O_3 is an important source for wintertime tropospheric O_3 in northern China and in the upper troposphere in southeast China while photochemical O_3 is responsible for the elevated O_3 observed in the BL of southeast China.

[25] **Acknowledgments.** This study is supported by grants from the Research Grant Council (RGC) of Hong Kong (PolyU 5061/99E and PolyU 5048/02E), an institutional research grant of the Hong Kong Polytechnic University (ASD 502), and a joint research grant from the National Natural Science Foundation of China and RGC (40318001). The nine ozonesondes launched in Hong Kong during PEACE-A period were provided by the National Space Development Agency of Japan. We thank the Director of Hong Kong Observatory and the Laboratory for Middle Atmosphere and Global Environment Observation, Institute of Atmospheric Physics, China, for their support and help in ozonesonde launching in Hong Kong and

Beijing, respectively. The authors would like to thank Isobel Simpson for her helpful comments on the paper.

References

- Angle, R. P., and H. S. Sandhu (1988), Urban and rural ozone concentrations in Alberta, Canada, *Atmos. Environ.*, *23*, 215–221.
- Austin, J. F., and R. P. Midgley (1994), The climatology of the jet stream and stratospheric intrusions of ozone over Japan, *Atmos. Environ.*, *28*, 39–52.
- Chan, C. Y., and L. Y. Chan (2000), The effects of meteorology and air pollutant transport on ozone episodes at a subtropical coastal Asian City, Hong Kong, *J. Geophys. Res.*, *105*, 20,707–20,719.
- Chan, C. Y., L. Y. Chan, Y. G. Zheng, J. M. Harris, S. J. Oltmans, and S. Christopher (2001), Effects of 1997 Indonesian forest fires on tropospheric ozone enhancement, radiative, and temperature change over the Hong Kong region, *J. Geophys. Res.*, *106*, 14,875–14,885.
- Chan, C. Y., L. Y. Chan, K. S. Lam, Y. S. Li, J. M. Harris, and S. J. Oltmans (2002), Effects of Asian air pollution transport and photochemistry on carbon monoxide variability and ozone production in subtropical coastal south China at Hong Kong, *J. Geophys. Res.*, *107*(D24), 4746, doi:10.1029/2002JD002131.
- Chan, C. Y., L. Y. Chan, W. L. Chang, Y. G. Zheng, H. Cui, X. D. Zheng, Y. Qin, and Y. S. Li (2003a), Characteristics of a tropospheric ozone profile

- and implications on the origin of ozone over subtropical China in spring 2001, *J. Geophys. Res.*, *108*(D20), 8800, doi:10.1029/2003JD003427.
- Chan, C. Y., L. Y. Chan, J. M. Harris, S. J. Oltmans, D. R. Blake, Y. Qin, Y. G. Zheng, and X. D. Zheng (2003b), Characteristics of biomass burning emission sources, transport, and chemical speciation in enhanced springtime tropospheric ozone profile over Hong Kong, *J. Geophys. Res.*, *108*(D1), 4015, doi:10.1029/2001JD001555.
- Chan, L. Y., H. Y. Liu, K. S. Lam, T. Wang, S. J. Oltmans, and J. M. Harris (1998), Analysis of the seasonal behavior of tropospheric ozone at Hong Kong, *Atmos. Environ.*, *32*, 159–168.
- Chan, L. Y., C. Y. Chan, H. Y. Liu, S. Christopher, S. J. Oltmans, and J. M. Harris (2000), A case study on the biomass burning in Southeast Asia and enhancement of tropospheric ozone over Hong Kong, *Geophys. Res. Lett.*, *27*, 1479–1483.
- Chan, L. Y., Y. M. Liu, S. C. Lee, and C. Y. Chan (2002), Carbon monoxide levels measured in major commuting corridors covering different landuse and roadway microenvironments in Hong Kong, *Atmos. Environ.*, *36*, 255–264.
- Eliassen, A. (1987), Entropy coordinates in atmospheric dynamics, *Z. Meteorol.*, *37*, 1–11.
- Fishman, J., and V. G. Brackett (1997), The climatological distribution of tropospheric ozone derived from satellite measurements using version 7 Total Ozone Mapping Spectrometer and Stratospheric Aerosol and Gas Experiment data sets, *J. Geophys. Res.*, *102*, 19,275–19,278.
- Folkens, I., and C. Appenzeller (1996), Ozone and potential vorticity at the subtropical tropopause break, *J. Geophys. Res.*, *101*, 18,787–19,792.
- Holton, J. R., P. H. Haynes, M. E. McIntyre, A. R. Douglass, R. B. Rood, and L. Pfister (1995), Stratospheric-tropospheric exchange, *Rev. Geophys.*, *33*, 403–439.
- Kajii, Y., K. Someno, H. Tanimoto, J. Hirokawa, H. Akimoto, T. Katsuno, and J. Kawara (1998), Evidence for the seasonal variation of photochemical activity of tropospheric ozone, Continuous observation of ozone and CO at Haplo, Japan, *Geophys. Res. Lett.*, *25*, 3505–3508.
- Kim, Y. K., H. W. Lee, J. K. Park, and Y. S. Moon (2002), The stratospheric-tropospheric exchange of ozone and aerosols over Korea, *Atmos. Environ.*, *36*, 449–463.
- Komhyr, W. D., R. A. Barnes, G. B. Brothers, J. A. Lathrop, and D. P. Opperman (1995), Electrochemical concentration cell ozonesonde performance evaluation during STOIC 1989, *J. Geophys. Res.*, *100*, 9231–9244.
- Lam, K. S., T. J. Wang, L. Y. Chan, T. Wang, and J. M. Harris (2001), Flow patterns influencing the seasonal behavior of surface ozone and carbon monoxide at a coastal site near Hong Kong, *Atmos. Environ.*, *35*, 3121–3135.
- Leung, Y. K., W. L. Chang, and Y. W. Chan (2004), Some characteristics of ozone profiles above Hong Kong, *Meteorol. Atmos. Phys.*, doi:10.1007/s00703-003-0052-9, in press.
- Liu, C. M., and H. W. Chang (2001), Characteristics of tropospheric column ozone over Taiwan, *Terr. Atmos. Oceanic Sci.*, *12*, 365–376.
- Luo, C., et al. (2000), A nonurban ozone air pollution episode over eastern China: Observation and model simulations, *J. Geophys. Res.*, *105*, 1889–1908.
- Ma, J., H. Liu, and D. Hauglustaine (2002), Summertime tropospheric ozone over China simulated with a regional chemical transport model: 1. Model description and evaluation, *J. Geophys. Res.*, *107*(D22), 4660, doi:10.1029/2001JD001354.
- Mauzerall, D. L., D. Narita, H. Akimoto, L. Horowitz, S. Walters, D. A. Hauglustaine, and G. Brasseur (2000), Seasonal characteristics of tropospheric ozone distribution and mixing ratios over east Asia: A global three-dimensional chemical transport model analysis, *J. Geophys. Res.*, *105*, 17,895–17,910.
- McPeters, R. D., G. J. Labow, and B. J. Johnson (1997), An SBUV ozone climatology for balloonsonde estimation of total ozone column, *J. Geophys. Res.*, *102*, 8875–8885.
- Menon, S., J. Hansen, L. Nazarenko, and Y. Luo (2002), Climate effects of black carbon aerosols in China and India, *Science*, *297*, 2250–2253.
- Murayama, S., K. Yamazaki, T. Nakazawa, and S. Aoki (1998), Interpretation of high mixing ratios of O₃ observed in the upper troposphere over Syowa Station, Antarctica using a trajectory analysis, *Geophys. Res. Lett.*, *25*, 1177–1180.
- Newell, R. E., E. V. Browell, D. D. Davis, and S. C. Liu (1997), Western Pacific tropospheric ozone and potential vorticity: Implications for Asian pollution, *Geophys. Res. Lett.*, *24*, 2733–2736.
- Oltmans, S. J., et al. (2001), Ozone in the Pacific tropical troposphere from ozonesonde observations, *J. Geophys. Res.*, *106*, 32,503–32,525.
- Oltmans, S. J., et al. (2004), Tropospheric ozone over the North Pacific from ozonesonde observations, *J. Geophys. Res.*, *109*, D15S01, doi:10.1029/2003JD003466.
- Parrish, D. D., Y. Kondo, O. R. Cooper, C. A. Brock, D. A. Jaffe, M. Trainer, G. Hübler, and F. C. Fehsenfeld (2004), Intercontinental Transport and Chemical Transformation 2002 (ITCT 2K2) and Pacific Exploration of Asian Continental Emission (PEACE) experiments: An overview of the 2002 winter and spring intensives, *J. Geophys. Res.*, *109*, D23S01, doi:10.1029/2004JD004980, in press.
- Pochanart, P., J. Hirokawa, Y. Kajii, H. Akimoto, and M. Nakao (1999), Influence of regional-scale anthropogenic activity in northeast Asia on seasonal variations of surface ozone and carbon monoxide observed at Oki, Japan, *J. Geophys. Res.*, *104*, 3621–3631.
- Shapiro, M. A., E. R. Reiter, R. D. Cadle, and W. A. Sedlacek (1982), Nowcasting the position and intensity of jet streams using a satellite-borne total ozone mapping spectrophotometer, in *Nowcasting*, edited by K. A. Browning, pp 137–145, Academic, San Diego, Calif.
- Sunwoo, Y., V. R. Kotamarithi, and G. R. Carmichael (1992), The regional distribution of tropospheric ozone in east Asia from satellite-based measurements, *J. Atmos. Chem.*, *14*, 285–295.
- Sunwoo, Y., G. R. Carmichael, and H. Ueda (1994), Characteristics of background surface ozone in Japan, *Atmos. Environ.*, *28*, 25–37.
- Tanimoto, H., O. Wild, S. Kato, H. Furutani, Y. Makide, Y. Komazaki, S. Hashimoto, S. Tanaka, and H. Akimoto (2002), Seasonal cycles of ozone and oxidized nitrogen species in northeast Asia: 2. A model analysis of the roles of chemistry and transport, *J. Geophys. Res.*, *107*(D23), 4706, doi:10.1029/2001JD001497.
- Tsutsumi, Y., and Y. Makino (1995), Vertical distribution of the tropospheric ozone over Japan: The origin of the ozone peaks, *J. Meteorol. Soc. Jpn.*, *73*, 1041–1058.
- Uccellini, L. W., D. Keyser, K. F. Brill, and C. H. Wash (1985), The Presidents' Day Cyclone of 18–19 February 1979: Influence of upstream trough amplification and associated tropopause folding on rapid cyclogenesis, *Mon. Weather Rev.*, *113*, 962–988.
- United Nations Environment Programme and Centre for Clouds, Chemistry and Climate (2002), *The Asian Brown Cloud: Climate and Other Environmental Impacts*, Nairobi.
- Wang, T., T. F. Cheung, M. Anson, and Y. S. Li (2001), Ozone and related gaseous pollutants in the boundary layers of eastern China: Overview of the recent measurements at a rural site, *Geophys. Res. Lett.*, *28*, 2373–2376.
- Wang, T., C. N. Poon, Y. H. Kwok, and Y. S. Li (2003), Characterizing the temporal variability and emission patterns of pollution plumes in the Pearl River Delta of China, *Atmos. Environ.*, *37*, 3539–3550.
- Yeung, K. K., W. L. Chang, R. E. Newell, W. Hu, and G. L. Gregory (1996), Tropospheric ozone profile over Hong Kong, *Meteorol. Soc. Bull.*, *6*, 3–12.
- Yonemura, S., H. Tsuruta, S. Kawashima, S. Sudo, L. C. Peng, L. S. Fook, Z. Johar, and M. Hayashi (2002), Tropospheric ozone climatology over Peninsular Malaysia from 1992 to 1999, *J. Geophys. Res.*, *107*(D15), 4229, doi:10.1029/2001JD000993.
- Zhang, M., I. Uno, S. Sugata, Z. Wang, D. Byun, and H. Akimoto (2002), Numerical study of boundary layer ozone transport and photochemical production in east Asia in the wintertime, *Geophys. Res. Lett.*, *29*(11), 1545, doi:10.1029/2001GL014368.
- Zhao, J., and K. S. Gallagher (2003), Clean vehicle development in China, *Sinosphere*, *6*, 20–28.
- Zheng, X. (2000), Analysis on the variations of tropospheric ozone vertical distribution, Ph.D. thesis, Peking Univ., Beijing, June.
- Zheng, X., W. Li, X. Zhou, J. Tang, and Y. Qin (2001), An analysis on the secondary ozone peak in the upper troposphere over Beijing in the summer of 1999 (in Chinese), *Adv. Nat. Sci.*, *11*(11), 1181–1185.
- Zheng, X., G. Ding, M. Sun, S. Li, J. Gong, W. Guo, and X. Wang (2002), Preliminary analysis on boundary layer ozone vertical profiles observed in winter in Beijing urban region (in Chinese), *Q. J. Appl. Meteorol.*, *13*, 100–108.
- Zhou, X., C. Luo, W. Li, and J. Shi (1995), The variation of total ozone in China and unusual ozone depletion center over Tibetan plateau (in Chinese), *Chin. Sci. Bull.*, *40*, 1396–1398.
- Zou, H. (1996), Seasonal variation and trends of TOMS ozone over Tibet, *Geophys. Res. Lett.*, *23*, 1029–1032.

D. R. Blake, Department of Chemistry, University of California, Irvine, CA 92697-2025, USA. (drblake@uci.edu)

C. Y. Chan, L. Y. Chan, H. Cui, H. M. Lam, Y. S. Li, and T. Wang, Department of Civil and Structural Engineering, Hong Kong Polytechnic University, Hung Hom, Hong Kong, China. (ceceychan@polyu.edu.hk; celychan@polyu.edu.hk; cecuih@polyu.edu.hk; cetwang@polyu.edu.hk)

E. W. L. Ginn and Y. K. Leung, Hong Kong Observatory, 134A Nathan Road, Kowloon, Hong Kong, China. (eginn@hko.gov.hk)

Y. Qin, C. S. Zhao, and Y. G. Zheng, Department of Atmospheric Sciences, School of Physics, Peking University, Beijing 100871, China. (qinyu@pku.edu.cn; zcs@pku.edu.cn; zhengyg@pku.edu.cn)

X. D. Zheng, Chinese Academy of Meteorological Sciences, Beijing 10081, China. (zhengxd@cma.gov.cn)

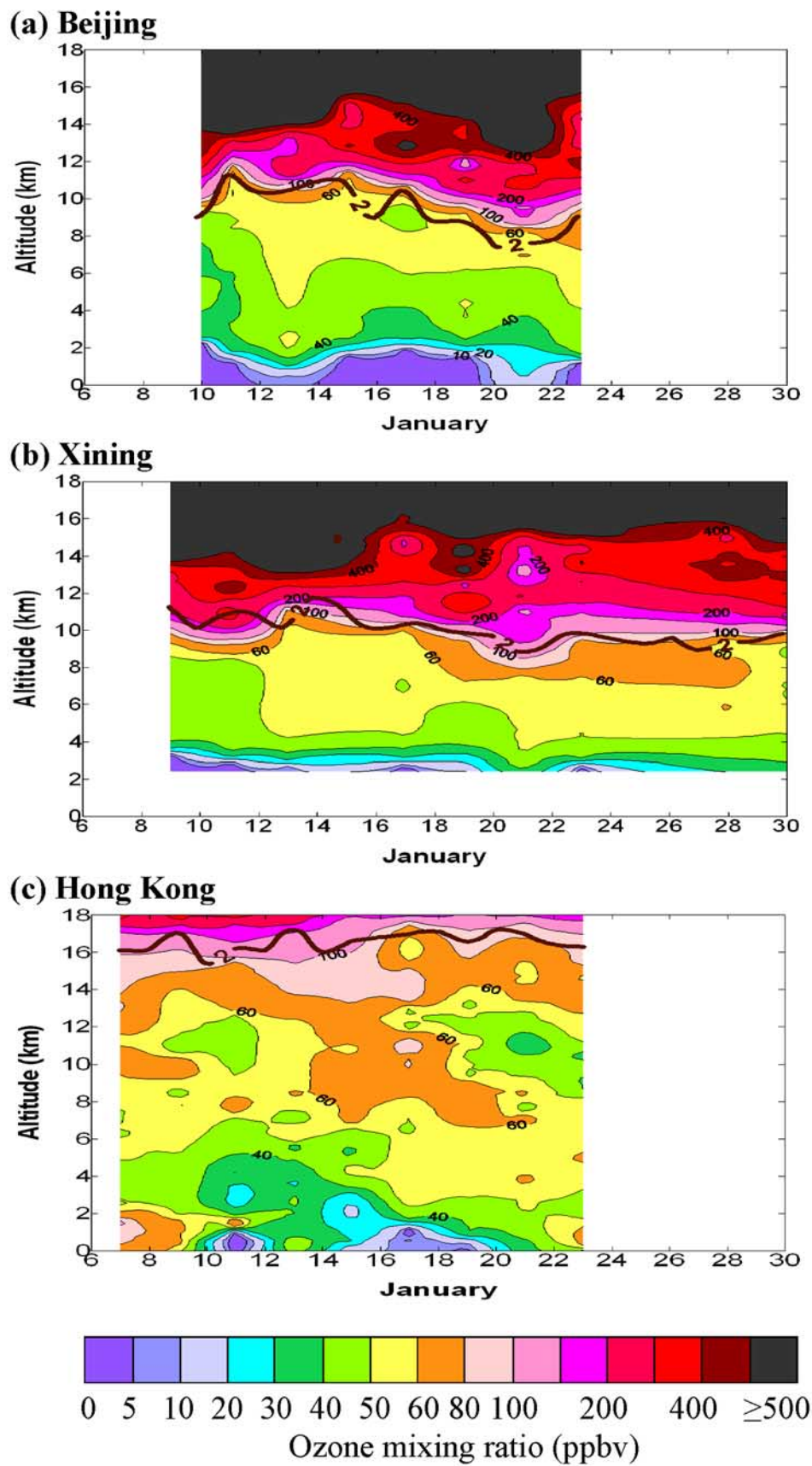


Figure 2. Time-height contour of ozone mixing ratio (ppbv) for (a) Beijing, (b) Xining, and (c) Hong Kong during the PEACE-A period. The dynamical tropopauses are identified by 2 unit lines of potential vorticity (PVU, $1 \text{ PVU} = 1 \times 10^{-6} \text{ s}^{-1} \text{ m}^2 \text{ kg}^{-1}$).

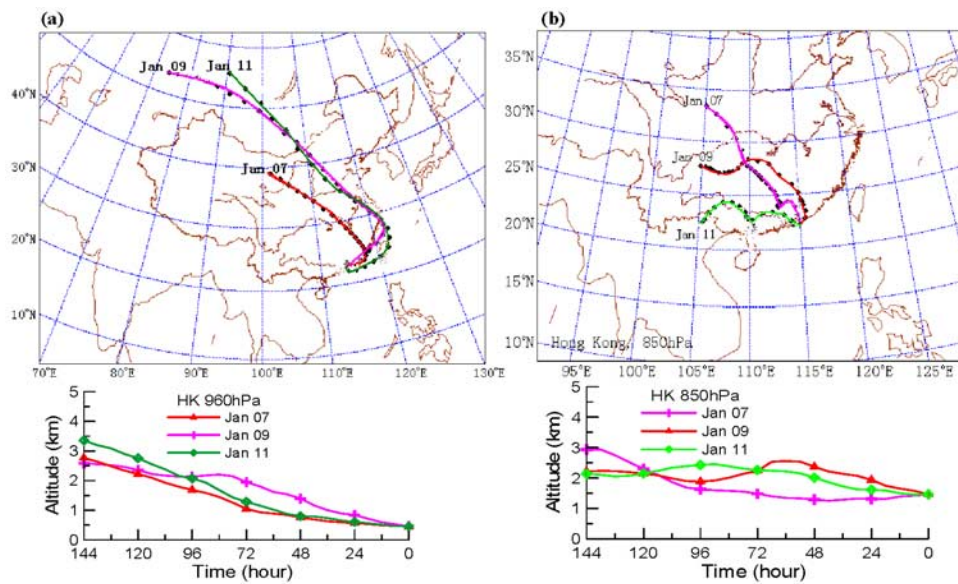


Figure 5. Five-day backward air trajectories reaching Hong Kong at (a) 960 hPa (~0.5 km) and (b) 850 hPa (~1.5 km) on 7, 9, and 11 January 2002.

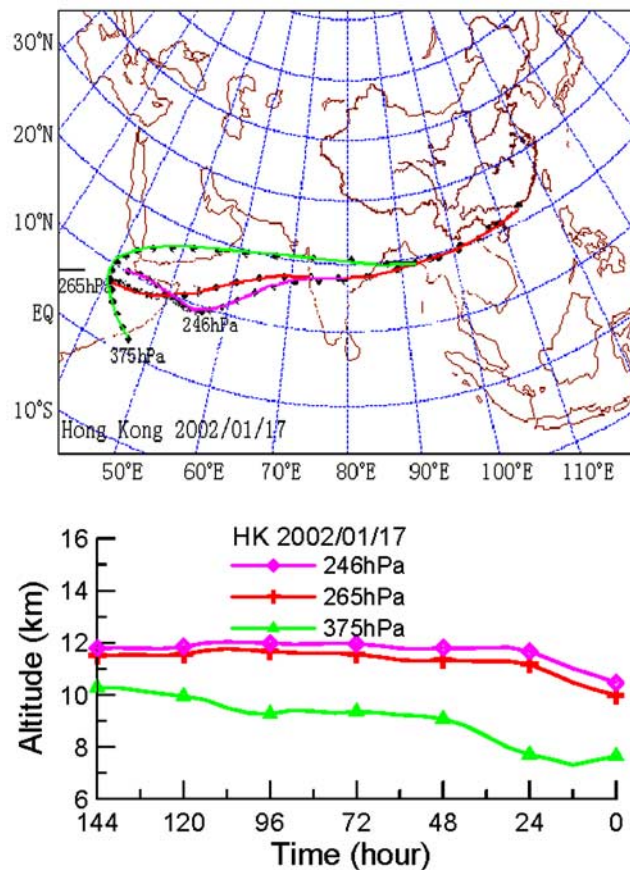


Figure 7. Five-day backward air trajectories reaching Hong Kong at 375, 265, and 246 hPa on 17 January 2002.

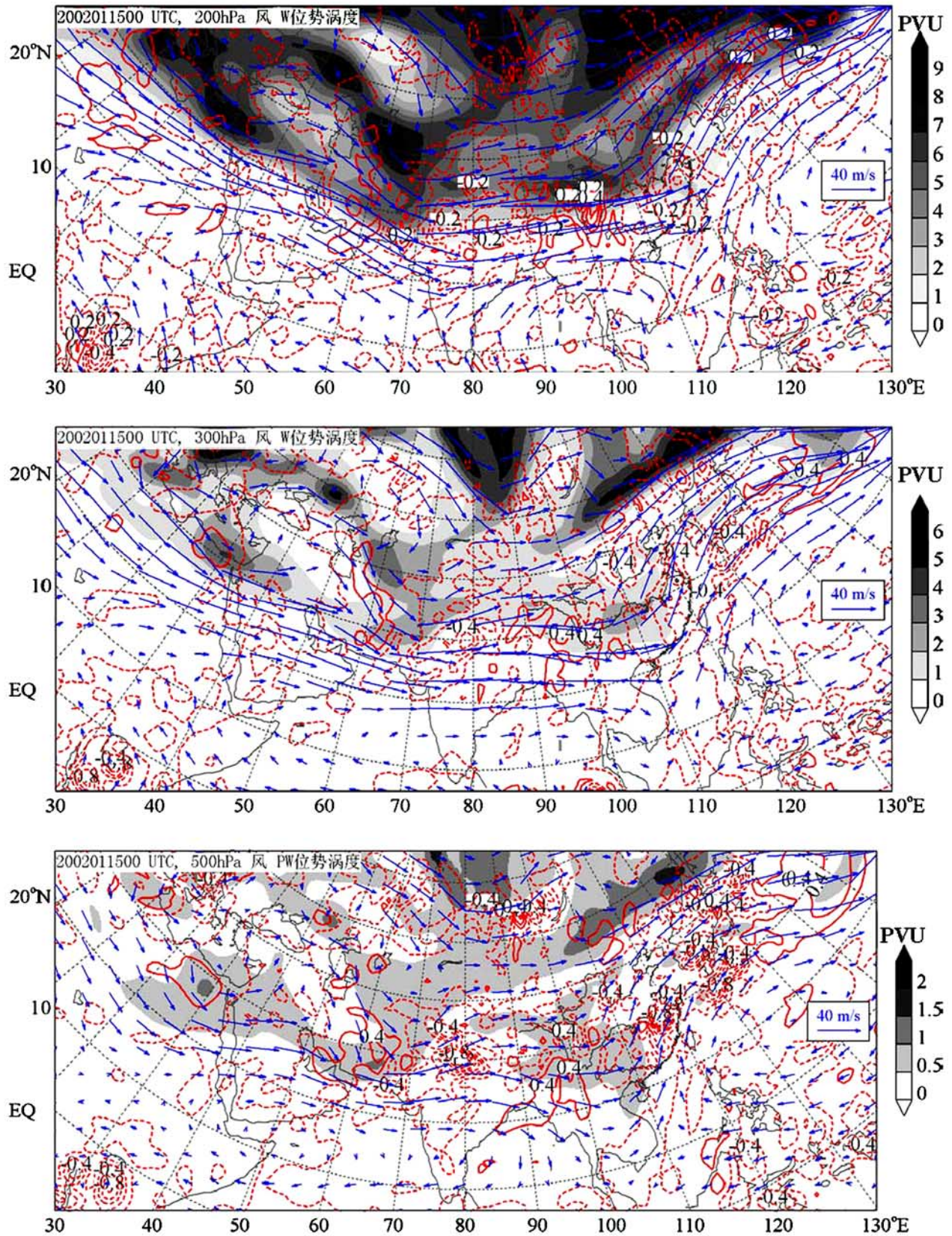


Figure 8. Distribution of potential vorticity (PVU) (shaded), pressure vertical velocity (Pa/s) (solid lines for positive, downward motion and dashed lines for negative, upward motion), and wind vector (m/s) (arrows) over Asia at 200, 300, and 500 hPa on 15 January 2002.

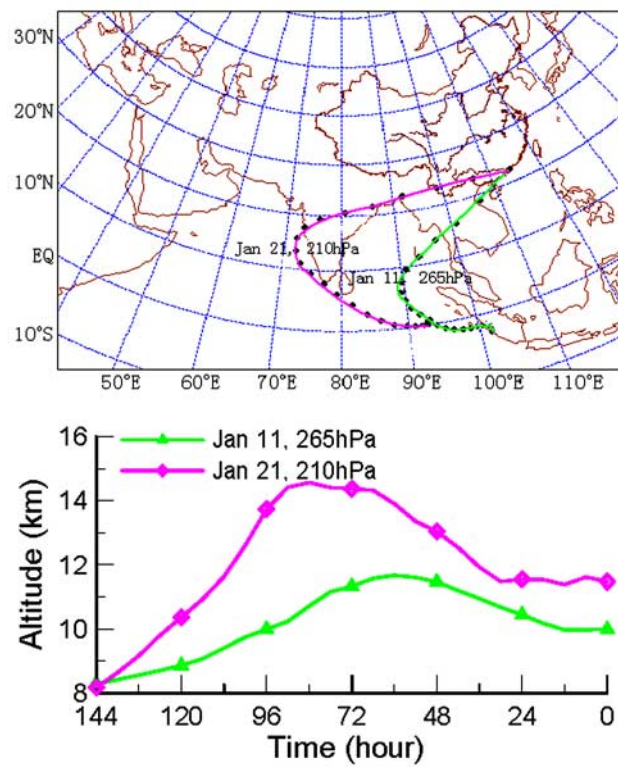


Figure 9. Five-day backward air trajectories reaching Hong Kong at 265 hPa on 11 January 2002 and at 210 hPa on 21 January 2002.

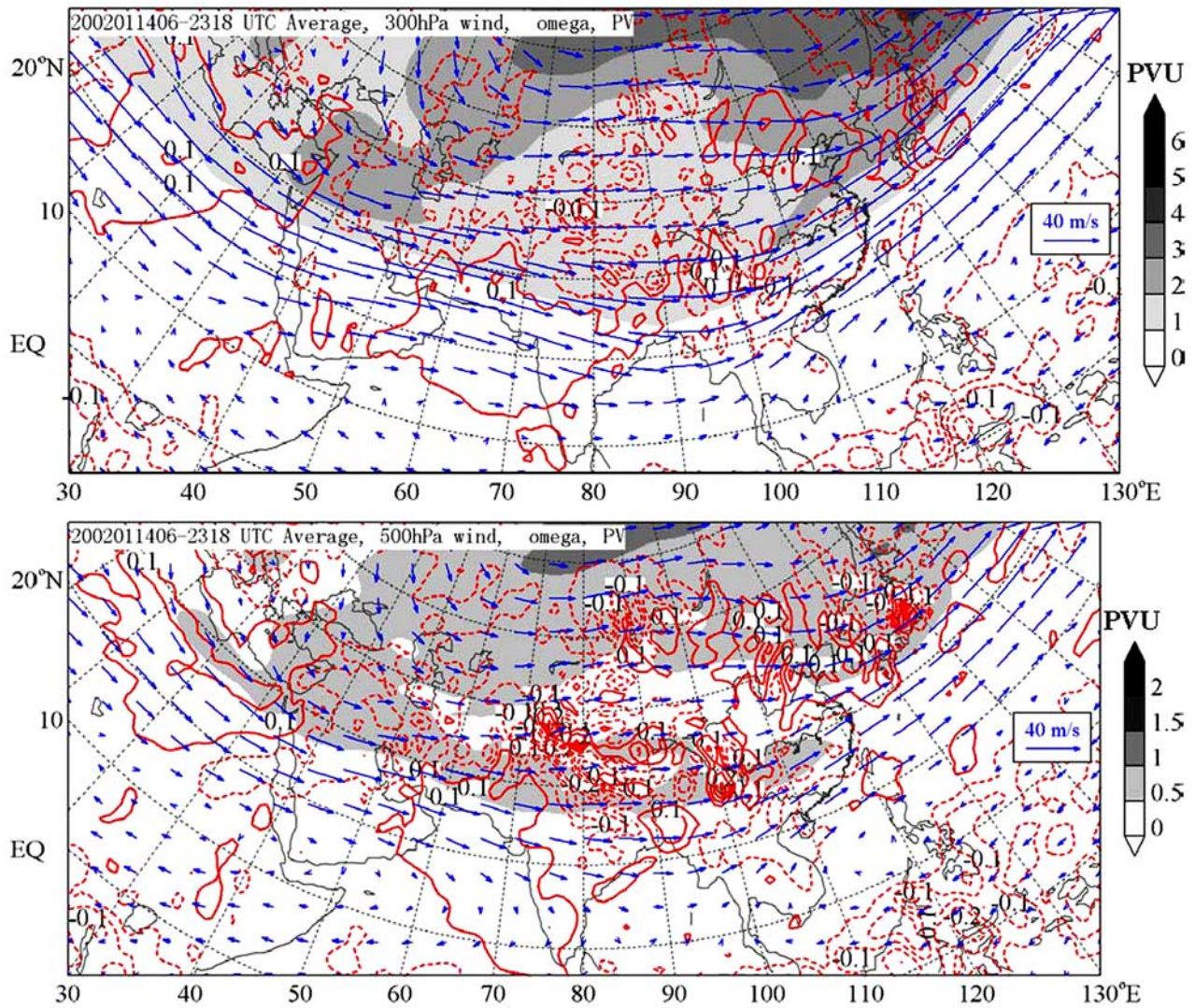


Figure 11. Mean potential vorticity (PVU) (shaded), pressure vertical velocity (Pa/s) (solid lines for positive, downward motion and dashed lines for negative, upward motion), and wind vector (m/s) (arrows) over Asia at 500 and 300 hPa averaged over the period from 6 to 23 January 2002.